Delta University Scientific Journal
Journal home page: https://dusj.journals.ekb.eg

Dish/Stirling Concentrated Solar Power Plant for Smart Grid Power Generation: Field Testing, Operational Experience, and Dynamic Performance Modeling

Mohamed E. Zayed[1], Jun Zhao[2], and A. E. Kabeel[1]
[1]*Department of Mechanical Power Engineering, Faculty of Engineering, Tanta University, Tanta 31521, Egypt.*
[2] *Key Laboratory of Efficient Utilization of Low and Medium Grade Energy, Tianjin University, MOE, Tianjin 300350, China*

Correspondence: [Mohamed E. Zayed.]; [RXGV+6P2, Sabarbay, Tanta, Gharbia Governorate 6646210.]; Tel [+20 1015363843]; Email: mohamed_zayed@f-eng.tanta.edu.eg

ABSTRACT
The use of solar-powered Stirling engines to convert thermal energy into electricity is a promising and renewable technological solution that can contribute to reducing dependence on fossil fuels for electricity generation. Unfortunately, the lack of experimental performance data and operating parameters for this type of technology limits its detailed characterization, difficult its modeling and design, and consequently its utilization. This paper aims to introduce an experimental analysis and mathematical modeling of a 1.5 MWe dish/Stirling concentrated solar power plant (DSCSPP), installed at Maricopa, Arizona, USA (33.0581° N, 112.0476° W). The daily, monthly, and annual performances of the DSCSPP are analyzed for one complete year to predict the annual electricity production. For daily summer conditions, the DSCSPP generates a peak electric power of 1.27 MWe at a direct solar irradiance (DNI) of 998 W/m2 with an overall plant efficiency of 23.7%. The results show that for DNI values between 472 and 998 W/m2, the experimental tests and the finding of the mathematical modeling do not present considerable differences, obtaining hourly electric power between 1.27 and 0.301 MWe which represents deviations in the range of 0.013%–16%. Moreover, the proposed DSCSPP produces 2550 MWh annually, with a yearly net overall efficiency of 17.8%.
Keywords: *Dish Stirling concentrated solar power plant; Experimental Implementation; Mathematical dynamic modeling; Performance prediction.*

1. Introduction

In recent years, the energy demand increasing has been one of the crucial challenges in this modern era, due to the rapid world overpopulation and water pollution aggravation (S.A. El-Agouz et al.) The use of renewable energy sources along with energy-saving measures is the main route to decarbonizing the energy sector (L. Jing et al.). Solar energy which is of a tremendous amount and entirely green entices many researchers to exploit proper techniques for the realization of highly efficient and clean solar energy usage such as photovoltaic systems (M.M. Aboelmaaref et al.), solar power generation (M.E. Zayed et al.), solar water desalination (M.E. Zayed et al.; D. Mevada et al.), absorption/adsorption devices and solar heating and cooling applications (S.M. Shalaby et al; M. E. Zayed etal). Solar power production systems use the sun as a heat source which can drive a heat engine for power generation by concentrated solar power technologies such as solar towers, parabolic dishes, parabolic troughs, and Fresnel reflectors (M.M. Aboelmaaref et al).
Dish/Stirling power system (DSPS) is one of the feasible solutions to convert solar energy into electricity with extra advantages such as high total efficiency, the variability of the heat source, and power capacity, and it has been successfully constructed and operated in several countries worldwide (M. E. Zayed et al.; R. Almodfer et al.). (Mancini et al) reviewed the technical specifications and performance behaviors of five types of standalone DSPS with rated powers between 9.5~25 kW and overall efficiencies values between 19.0%~29.4%. It was reported that the 25 kW DSPS, which was built by the Stirling Energy Systems (SES) company in Boeing, California, USA, achieved the highest efficiency (29.4%). A commercial DSPS was experimentally established and economically evaluated by (Zayed et al) in Tianjin, China. The daily, monthly, and yearly thermodynamic analyses of the DSPS were conducted for estimating annual energy output, the gross yearly efficiency, and the energy cost of the DSPS.

It was shown that the DSPS produced a yearly energy output of 28.748 MWh with a gross annual efficiency of 19.5 %, yielding an energy cost of 0.2565 $/kWh. (Buscemi et al) experimentally tested and theoretically modeled a 32 kW standalone DSPS in Palermo, Italy. A numerical approach for evaluating the daily effect of mirror soiling was also proposed. In March 2010, Maricopa DSCSPP in Arizona, USA was linked to the grid and installed by SES Co., which consisted of 60 dishes, each one having an electric power of 25 kW. This plant used silver glass parabolic mirrors with a reflectance of 94%. Maricopa DSCSPP produced electricity of 1.5 MW with 26% gross annual efficiency (NREL; SES). In the year 2012, a 100 kW DSCSPP was constructed by Great Ocean Energy Co., in Ordos city, Nei Mongolia, China with a unit capacity of 10 kW [18]. In 2013, a 1.0 MW Orion DSCSPP comprising eight identical dishes, has been established in Wuhai, Inner Mongolia, China. The Wuhai DSCSPP had an air receiver and reticulated hot air for centralized deriving of an ORC (J. Coventry et al). (Zayed et al) investigated the impact of the concentrator diameter, receiver operational temperature, DNI, wind speed, and ambient temperature on the SDSES's output power and total efficiency. The finding shows that the power output and overall efficiency of SDSS increase with increasing DNI and receiver temperature while decreasing with increasing ambient temperature and increasing wind speed. (Guarino et al) proposed a heat and electric power cogeneration plant implementing a field of dish-Stirling collectors, a seasonal geothermal storage, and a system of water-to-water heat pumps for the first time, which can cover 97% of the building's annual thermal loads with energy produced by the solar system with the best plant configuration.

On the other hand, some attempts have been performed using artificial neural methods (ANNs) to predict the performance of DSPS and minimize the high cost required for the construction and testing of these systems (S.A. El-Agouz et al). (Loni et al) used the Data Handling Group Method (DHGM) to predict the thermal efficiency and cavity heat gain of a hemispherical receiver combined with a dish collector. The outlet temperature, direct irradiance, and weather temperature were selected as inputs. It was indicated that the R2 values for the efficiency and heat gain of the cavity based on the DHGM model were 0.9567 and 0.9709, respectively. (M. Ahmadi et al) proposed a feed-forward ANN integrated with an optimization algorithm that involved a combination of genetic algorithm and particle swarm optimization (PSO) to forecast the electrical power and total efficiency of the DSPS. (Alata et al) proposed a diffuse control solar tracking system using the adaptive neuro-fuzzy inference system (ANFIS) to maximize the solar intensity incident on a focal plane surface. (Khosravi et al) developed three different hybrid artificial intelligence methods namely; MLP-ANN, DHGM, and ANFIS to assess the effect of various geometrical and operative parameters on the produced power and efficiency of the DSPS, considering Natal, Brazil as a case study. The ANN and ANFIS were optimized with GA and PSO. It was clarified that the statistical results unveiled that the ANFIS integrated PSO approach yielded the best performance among the studied intelligence approaches.

A solar dish/Stirling power plant (DSCSPP) consists of several arrays of dish/Stirling units in the same location, in which each dish unit is designed with the same size and unit-rated capacity to produce electricity. The performance of DSCSPP is affected by various regional features and variables such as climatic features, geographic attributes, and government financial incentives, as well as several complicated parameters such as the side and back distances between dish units, the number of units in each array, the shadow effect, the influence of mirrors soiling coefficient of the concentrators, which causes a change in the instantaneous electrical power produced from one unit to another. Different standalone configurations of the dish/Stirling systems have been studied and analyzed with the main results published in the specialized literature, but there are few studies around the world have been conducted, to investigate the performance and evaluate the electricity generation of solar dish power plants. Moreover, there are few studies on the combined application of power and heat in the solar dish system, which is mainly due to the limitations of the PCU of the solar dish system, i.e., the Stirling engine. The contribution and novelty of this work are to present the experimental implementation, mathematical modeling, and thermodynamic evaluation of a dish/Stirling concentrated solar power plant (DSCSPP) using data obtained from experimental tests of Maricopa DSCSPP, Arizona, USA (33.0581° N, 112.0476° W, besides presenting geometric and operating parameters of this type of sustainable power plant technology. Moreover, the proposed DSCSPP is modeled and simulated based on MATLAB software to predict and estimate the hourly, monthly, and annual energy output. The daily, monthly, and annual performances of the DSCSPP are extensively analyzed for one complete year to predict the annual electricity production.

2. Material and methods

To verify the accuracy of the proposed mathematical model developed in this study, experimental data from the literature were used, in which the thermal behavior of real DSCSPP is considered. More specifically, the practical measurements of the Maricopa DSCSPP in Arizona, USA, taken from the SES-2013 technical report (NREL; SES), are used in this study

2.1. Dish/Stirling Solar Power Plant Description

The Maricopa DSCSPP is a 1.5 MW CSP project in Arizona, USA, and it is regarded as the world's first commercial DSCSPP to manifest the novel sun catcher technology. The plant launched its operation in December 2009 and officially began in January 2010. The plant was installed and owned by SES Inc. Co. and Texas-based Tessera solar partner. The Maricopa DSCSPP was providing electricity to the state-owned Salt River Project in Phoenix district, USA. It was comprised of 60 dishes as clearly presented in Fig. 1 (a). In this plant, each dish unit was called the Sun-CatcherTM system, which was a 25 kW modular electrical power conversion system that harvests solar energy and converts it into AC electric power utilizing a dish concentrator and power conversion unit (PCU) as seen in Fig. 1 (b). A detailed schematic diagram for the sun-catcher DSPS components. The dish concentrator of the sun-catcher system was 10.73 m in diameter, and which built of an array of 44 precisely-aligned mirror facets with reflectivity of 94 %, which were attached to the facet support structure (FSS). The FFS was comprised of a steel framework structure of trusses and cross-joints that carries the facets of the mirror, as well as forming the structural integrity of the DSPS.

The Sun-Catcher unit system used a Kockums 4-95 Stirling PCU, which is considered the world's leader in kinematics SE. The subsystems of the Kockums 4-95 Stirling PCU were:

- Direct illumination receiver was comprised of an isolated cavity receiver with an aperture to permit the concentrated energy to get through the cavity, which includes the four heater heads of the SE. Each heater head was a bundle of tubes, which contains hydrogen as working gas.
- Kockums kinematics SE was a four-cylinder reciprocating engine with a displacement of 380 cm3, receiving heated and compressed hydrogen gas from the cavity receiver to power the SE cycle.
- Electrical generator that converted the mechanical energy to electrical energy;
- The cooling system that rejected waste heat to the surrounding by using a water radiator;
- Control system that monitored and controlled system operation; and
- Support frame that attached the SE assembly to the boom, and the boom permits for the PCU mounting so that the PCU is in the perfect positioning relative to the facets of the mirror, as shown in Fig.1 (c). The parabolic concentrator focuses sunlight on the PCU aperture which then significantly heats the hydrogen gas in heater head tubes of SE to 700 ºC and the heated gas runs through a heat exchanger to drive the SE. Then, the SE powers a 3 w/480v/Induction generator to produce electricity. The AC power produced by the PCU was fed through electrical cables to a connector box, which connected the electrical power to the grid. In addition, the FSS and boom used a joint mounting hub. The hub and boom allowed mounting provisions for both motor drives (elevation drive and azimuth tracking). The FSS, boom, hub, and mirror facets all form the dish concentrator structure. The dish also utilized a 2-D axis tracking system to track the sun accurately. The tracking system was a conjunction of the azimuth angle rotating mechanism and screw expand and contract mechanism. Moreover, a tubular pedestal assembly was also installed to hold the dish concentrator at a constant height from the ground.

Fig. 1 (a) Overview of the Maricopa DSCSPP, Peoria, Arizona, USA (J. Coventry et al); (b) Commercial unit-scale Sun Catcher DSPS for the Maricopa DSCSPP (V. Visa et al); (c) View of the PCU for the unit-scale Sun Catcher DSCSPS.

2.2. Measurement Techniques and Experimental procedures

An extensive measurement campaign was carried out to collect data related to the operation of the Maricopa DSCSPP Peoria, Arizona, USA, in the period between March 2010 and July 2011. During this period, the full operation of the solar plant was interrupted one time due to the maintenance and testing stages planned for the DSCSPP. The performance of the DSCSPP was daily examined under different conditions of solar irradiance, airspeed, air temperature and relative humidity from 7:00 am to 7:00 pm. The main physical quantities recorded during this stage were: the net electrical power output using an energy meter (ABB - A43 212–100, with an accuracy of the active and reactive energy class of ±1% and ±2% respectively). Also, the solar beam radiation Gbn was recorded using a pyrheliometer (Kipp&Zonen -SHP, with an average accuracy of ±0.5%) and the external ambient temperature Tamb using a weather transmitter (Vaisala – WXT536 with an accuracy of ±0.3 °C at + 20 °C). The other most relevant physical quantities measured in the same period were the limiting temperatures of the Stirling engine Th and Tc, which were measured by a VDO Pyrometer thermocouple probe 900°C - R ¼, ±0.10 °C.

The originally measured quantities were collected with a one-second temporal resolution in a MySQL database consisting of 14,256,000 records. The data was preliminarily filtered to avoid points representing mechanical transients. Thus, considering that the sampling frequency of the signals coming from the dish-Stirling plant is 1 Hz, it was first necessary to define a "moving average filter" procedure useful for both the reduction of the quantity of data and the filtering of the transients. Utilizing the mentioned accuracies of the utilized instruments in this work, the relative error in the electric power production of the unit system of DSCSPP is computed utilizing the error analysis given by (Holman) procedure which is found to be 4.47%.

2.3. Mathematical Modeling

In this study, a new algorithm consisting of three sub-models implemented in MATLAB software for analyzing the DSCSPP performance is proposed. The first model is used to calculate the geometrical parameters such as focal length, receiver diameter, concentrator efficiency, and the distance of the receiver from the focus point for the geometrical dish configuration of the investigated DSPS. While, the second one is a comprehensive thermodynamic model that is used to evaluate the daily, monthly, and annual performances of the investigated DSCSPP.

2.3.1. Opt-geometric Model

This model is used to calculate the geometrical parameters of each dish unit for the DSCSPP, which is consisted of 60 dishes such as receiver diameter, focal length, design geometric concentration ratio, and the distance of the receiver from the focus point. Fig. 2 shows different geometrical parameters of the concentrator/receiver system such as the rim angle "**φ**r", focal length "f", the receiver optimal height "H_r", the diameter of dish concentrator "Dc", the distance of the focus point from the receiver "df", the lateral distance between the concentrator surface and the focus point of receiver "P", and the receiver diameter "D_r".

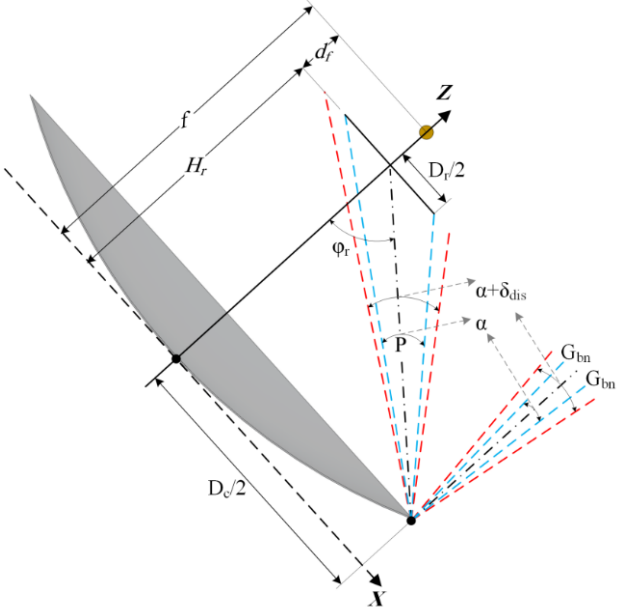

Fig. 2. Geometric distances and dimensions of the concentrator/receiver system.

In the concentrator/receiver system, the rim angle "**φ**$_r$" is defined as the angle between the axis and a line from the focus to the physical edge of the concentrator. The rim angle and focal length of a dish concentrator completely

define its cross-sectional geometry. In this study, a dish concentrator design with a rim angle of 45° has been proposed, as a means of obtaining the highest geometric concentration ratio "$C_{g,D}$" (P.R. Steinfeld et al.). The optimal height of receiver "$_{Hr}$" represents the position of the focal point, at which the direct solar irradiance concentrates in a single point reaching high temperatures, these temperatures damage the material of the receiver surface, where the working gas flows. Hence, the cavity receiver is designed to be at a distance "d_f" from the focus point to avoid the overheating of the cavity receiver material and ensure uniform direct solar radiation.

To determine the proper geometry of the concentrator/receiver of the proposed DSPS or any other DSPS, Table 1 presents the opto-geometric model manner that can be described as follows: first, the model has an input, which is the diameter of the concentrator, besides the concentrator's constants that define its optical performance and finally the most important equations to perform the Opto-geometric sizing of the DSPS (P.R. Steinfeld et al.).

2.3.2. Thermal Analysis Model

In a typical SDS system, there are three main energy forms subjected to different conversion schemes: solar energy, thermal energy, and electrical energy. As shown in Fig. 3, the received solar radiation by the concentrator surface is concentrated at a very high concentration ratio onto the receiver. The receiver loses heat in three different modes: conduction through its walls; convection to the surrounding air, and radiation from the aperture opening to the surrounding (] R. Beltrán-Chacon et al).

In the Stirling engine cycle, four different processes are constituted as follows:

i) An isothermal process (1–2), where the HTF releases the heat into the heat sink at a constant temperature, TL.
ii) In an isochoric process (2–3), the HTF passes through the regenerator and is heated up to Th.
iii) In an isothermal heat addition process (3–4), the HTF spreads out and acquires the heat from the heat source (thermal receiver).
iv) Finally, an isochoric process of cooling from (4–1), in which the regenerator extracts the heat from the HTF.

Therefore, a thermodynamic model was developed to evaluate the daily, monthly, and annual performances of the SDS system via predicting its output power and total efficiency. This may be achieved by calculating the useful energy gained by the system via calculating different losses and efficiencies at each stage of the system [27-30] under the following assumptions:

- Steady-state conditions under the energy flow scheme.
- The solar radiation is uniformly distributed on the cavity surface.
- The cavity wall temperature is equal to the operational temperature of the cavity receiver.

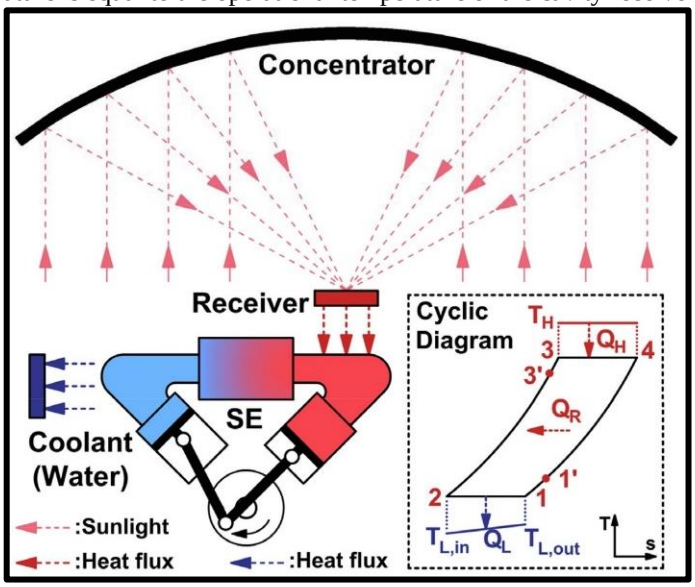

Fig. 3. Energy balance diagram of SDPS..

The useful energy Q_u has defined as the difference between the concentrated energy on the receiver surface Q_{con} and the total heat losses:

$$Q_u = Q_{con} - Q_{loss} \quad (8)$$

The concentrated energy on the receiver is given:

$$Q_{con} = \rho_m \Gamma G_{bn} A_c \quad (9)$$

Where ρm denotes the concentrator mirror reflectance, Γ denotes the solar interception factor (the ratio of the intercepted energy on the receiver surface to the reflected energy from the concentrator mirrors). It was reported that

the solar interception factor value varied from 0.9 to 0.99. Hence, in this paper, the interception factor value is assumed to be 0.9 to attain a critical condition of the concentrator/receiver system, at which the maximum possible amount of optical losses is taken into account. Where G_{bn} represents the direct solar radiation incident on the concentrator and A_c denotes the dish concentrator aperture area.

The radiative heat losses is composed of two components: reflected and emitted radiation:

$$Q_{rad} = Q_{rad,ref} + Q_{rad,emi} \quad (10)$$

The reflected radiation losses are given as (Z. Li et al);

$$Q_{rad,ref} = Q_{con}\left[1 - \alpha_{eff}\right] \quad (11)$$

Where αeff is the effective absorbance of the cavity that considers the multiple reflections inside the cavity, which can be calculated in terms of the diameters of the cavity and the receiver, the absorptivity of the receiver material (Z. Li et al);

$$\alpha_{eff} = 1 - \frac{\alpha_{abs,r}}{\alpha_{abs,r} + \left(1 - \alpha_{abs,r}\right)\frac{A_r}{A_{cav}}} \quad (12)$$

The emitted radiation losses are given as (Z. Li et al);

$$Q_{rad,emi} = \sigma\, \varepsilon_r\, A_r\, (T_{cav}^4 - T_\infty^4) \quad (13)$$

The total convective loss "Q_{conv}" is composed of two components: the natural convection heat loss and the forced convection heat loss.

$$Q_{conv} = \left(h_{conv,nat} + h_{conv,forced}\right) A_{cav}\, (T_{cav} - T_\infty) \quad (14)$$

The natural convective HTC depends on the diameters of the cavity and the receiver, the thermal conductivity of the receiver material, the tilt angle of the receiver, and the temperatures of the cavity and surroundings. It can be calculated as follow (M. Castellanos et al);

$$h_{conv,nat} = \frac{\lambda_r}{D_r}\left[0.088.Gr^{0.333}.\left(\frac{T_{cav}}{T_\infty}\right)^{0.18}.(\cos\phi)^{2.47}.\left(\frac{D_r}{D_{cav}}\right)^{1.12-0.98\left(\frac{D_r}{D_{cav}}\right)}\right] \quad (15)$$

The forced convective HTC can be calculated in terms of the receiver tilt angle ϕ and the wind speed v_w, as given by (R. Y. Ma et al);

$$h_{conv,forced} = f(\phi).v_w^{1.401} \quad (16)$$

Where f (ϕ) is defined as:

$$f(\phi) = 0.1634 + 0.7498\sin\phi - 0.5026\sin 2\phi + 0.3278\sin 3\phi \quad (17)$$

Herein, the tilt angle "ϕ" is defined as the inclination angle of the cavity receiver on the horizontal plane, and it was set at 75° as recommended by (G. Caballero et al), which induces low wind convection heat loss.

The conduction heat loss is given as [36];

$$Q_{cond} = \frac{(T_{cav} - T_\infty)}{\frac{ln\frac{D_{ro}}{D_{ri}}}{2\,\pi\,\lambda_r\,L_r} + \frac{ln\frac{D_{cav}}{D_{ro}}}{2\,\pi\,\lambda_{ins}\,L_{ins}} + \frac{1}{h_{ext,cav}\;A_{o,cav}}} \quad (18)$$

The convective HTC on the external surface of the receiver housing is given by (Morgan et al).

$$h_{ext,cav} = 0.148\, Re^{0.633}.\frac{\lambda_\infty}{D_{cav}} \quad (19)$$

To determine the receiver operating temperature, the empirical equation proposed by (Steinfeld and Schubnell) is adapted in this study considering the parameters as excess heat removal factor "F_{Ex}", degradation factor "FD", and the concentrator efficiency, to attain more relevance results with the real SDPS technologies. The concentrator efficiency is calculated based on the optical losses and the manufacturing errors of the concentrator, which are determined in the following subsection. The degradation factor which represents the errors related to the solar tracking system is set at 0.8 in this study (M. E. Zayed). While the excess heat removal factor takes into account the cavity overheating condition; as the receiver temperature exceeds a certain value, the excess heat is removed via a cooling fluid using a cooling system to maintain nominal operational temperatures. The cavity receiver temperature "T_{cav}", is given by (M. Castellanos et al);

$$T_{cav} = \sqrt[4]{\frac{\alpha_{abs,r}\;C_{g,D}\;G_{bn}}{\varepsilon_r\,\sigma}}.\xi_{att} \quad (20)$$

Where "ξatt" is an attenuation constant that represents all parameters used to maintain the receiver temperature close to the operating temperatures is given as:

$$\zeta_{att} = \eta_c\, F_D\, F_{Ex} \quad (21)$$

The concentrator efficiency η_c can be calculated in terms of concentrator mirrors materials properties and the errors in the mirror from the manufacturing process, as given by (M. Castellanos et al);

$$\eta_c = \rho_m\; F_s\, \Gamma \quad (22)$$

Where, ρ_m, F_s, and Γ denote the reflectance of concentrator mirrors, the dusting factor, and the solar interception factor, respectively.

The receiver thermal efficiency η_r is defined as the ratio between the useful thermal energy utilized in the Stirling engine and the solar energy concentrated on the receiver aperture and is given as (M. Castellanos et al);

$$\eta_r = \frac{Q_u}{Q_{con}} = \frac{Q_{con} - \sum Q_{loss}}{Q_{con}} = 1 - \frac{\sum Q_{loss}}{Q_{con}} \qquad (23)$$

Stirling engine efficiency is affected by the technological coefficient Ω_{St}, considering the irreversibility due to pressure losses and incomplete regeneration in the Stirling engine components and is given as (M. E. Zayed et al);

$$\eta_{st} = \Omega_{st}\left(1 - \frac{T_{f,com}}{T_{cav}}\right) \qquad (24)$$

Where Ω_{St}, represents Stirling constant, $T_{f,\,com}$ denotes the temperature of working fluid in compression space of Stirling Engine and T_{cav} denotes the cavity temperature.

Herein, in this paper, to validate the Stirling engine efficiency of the system, the value of the Stirling engine coefficient "Ω_{St}" is considered to be 0.55, according to (Kongtragool and Wongwises), taking into account the most unfavorable condition and simulating a critical condition SDS system, at which the maximum possible amount of incomplete regeneration and pressure losses that can be released from the Stirling engine are taken into account. Moreover, the temperature of the working fluid in the engine compression space is set at 390 K.

The overall efficiency of the unit SDPS system η_o is defined as the ratio of the generated electrical power produced to the solar energy concentrated on the receiver aperture to the globally available amount of solar energy falling on the concentrator and is given as:

$$\eta_o = (\rho_m\ F_{sh}\ \Gamma) * \left(1 - \frac{\sum Q_{loss}}{Q_{con}}\right) * \Omega_{st}\left(1 - \frac{T_{f,com}}{T_{cav}}\right) * \eta_{gen} \qquad (25)$$

The net electrical power generated from SDPS is calculated as:

$$P_e = \eta_o\ A_c\ G_{bn} \qquad (26)$$

Table 2 presents the operating conditions, weather variables, and the investigated SDPS own constants that define its opto-geometric configuration (estimated in the present study from the Opto-geometric sizing results), as well as the properties of the materials of system components that are mathematically used to evaluate the thermal performance of the SDSPS in the thermal analysis model.

TABLE 1 MAIN DATA AND EQUATIONS OF THE OPTO- GEOMETRIC MODEL.

Input data		
Dish concentrator diameter, m (D_c)		
Dish concentrator constant optical parameters		
Rim angle	φ_r	45°
Total optical error (mrad)	σ_t	8
Solar angle	α_s	0.53°
Dispersion angle	δ_{dis}	0.605°
Mathematical equations used to perform the opto-geometric sizing		
Focal length	$f = \frac{D_c}{4\tan\left(\frac{\varphi_r}{2}\right)}$	(1)
Lateral distance between the concentrator surface and the focal point of the receiver	$P = \frac{2f}{1+\cos\psi}$	(2)
Total beam spread perpendicular to the centerline of the reflected beam	$\Delta_{b,r} = 2P\tan\left(n\ \frac{\sigma_t}{2}\right)$	(3)
Diameter of the receiver	$D_r = \frac{\Delta_{b,r}}{Cos\,(\varphi_r)}$	(4)
Distance of the receiver behind the focus point	$d_f = \frac{D_r}{D_c}\left(f - \frac{D_c^2}{16\,f}\right)$	(5)
Optimum height of the focus point	$H_r = f - d_f$	(6)
Design geometric concentration	$C_{g,D} = \left[\frac{Sin\,\varphi_r\,Cos\left(\varphi_r + \frac{\delta_{dis}+\alpha_s}{2}\right)}{Sin\left(\frac{\delta_{dis}+\alpha_s}{2}\right)}\right]^2$	(7)

TABLE 2 INPUT DATA AND THE CONSTANT PARAMETERS OF THE PROPOSED SDPS USED IN THE THERMAL MODEL.

Input data		
Solar direct irradiation (G_{bn})	Ambient temperature (T_∞)	Wind speed (v_w)
Dish concentrator constant parameters		
Aperture diameter (m)	D_c	10.0
Intercept factor	Γ	0.9
Mirror reflectance	ρ_m	0.92
Design geometric concentration	$C_{g,D}$	2498
Un-shading factor	F_{sh}	0.9^{V}
Degradation factor	F_D	0.8
Cavity receiver constant parameters		
Receiver diameter (m)	D_r	0.2
Receiver absorptivity (%)	$\alpha_{abs,r}$	0.96
Receiver emissivity (%)	ε_r	0.85

Cavity thickness (mm)	L_r	3
Cavity insulation thickness (mm)	L_{ins}	75
Excess heat removal factor	F_{Ex}	0.5
Stirling engine and alternator constant parameters		
Stirling constant	Ω_{St}	0.55
Temperature of working fluid in the compression space of Stirling engine (K)	$T_{f,com}$	390
Alternator efficiency (%)	η_{gen}	0.9٢٥

Results and Discussion

In this work, the ability of the thermal analysis model for the prediction of instantaneous electrical power and monthly energy production of the DSCSPP is examined. In this work, the instantaneously measured data of the direct solar irradiance, the wind speed, the relative humidity, and the ambient temperature, as well as their corresponding electrical output power for the Maricopa DSCSPP, during the daytime operation period on 12 June 2010. In the same context, the monthly averagely recorded data of the direct solar irradiance, the wind speed, the relative humidity, and the ambient temperature, as well as their corresponding monthly energy produced for the Maricopa DSCSPP, in the period between March 2010 and June 2011, are also trained for prediction the monthly electrical energy. The measurements for the Maricopa DSCSPP that were used in this study were in the period between March 2010 and June 2011, and outdoor measurement tests were carried out to collect data related to the operation of the Maricopa DSCSPP. During these tests, the key performance parameters recorded instantaneously were: the gross electrical output power, the direct solar irradiance, wind speed, relative humidity, and the ambient temperature. In this work, the instantaneously measured data of the direct solar irradiance, the wind speed, the relative humidity, and the ambient temperature, as well as their corresponding electrical output power for the Maricopa DSCSPP, during the daytime operation period on 15 July 2010 (Fig. 5), are used to train the developed prediction model for prediction the instantaneous electrical rated power produced by the DSCSPP.

The thermal performance of the DSCSPP is experimentally tested considering a typical summer day in Arizona, USA (33.0581° N, 112.0476° W), in June 2010 from 7:00 to 19:00. Fig. 4 demonstrates the instantaneous recorded data of the direct solar irradiance, the wind speed, the relative humidity, and the ambient temperature. It is indicated the wind speed data of Maricopa City was measured with an average value of 5.05 mph for wind speed. The amount of direct solar radiation and the ambient temperature are plotted in Fig. 4. It also clearly shows that the average measured values of the direct solar irradiation and ambient temperature are 888 W/m2 and 33 oC, respectively. Fig. 7 also displays the instantaneous measured electrical power output of the DSCSPP during the daytime on June 12th. It is clear that in Fig. 4, the power output slightly changes in the midday period (10 a.m. - 3 p.m.) compared to other daytime periods, this is due to the slight change in the operating temperature in the midday period, as a result of the slight change of direct solar irradiance. It can be concluded that the maximum and average measured values of the output power for the investigated DSCSPP are found to be 1.27 MW and 1.10 MW, respectively.

On the other hand, the monthly averagely recorded data of the direct solar irradiance, the wind speed, the relative humidity, and the ambient temperature, as well as their corresponding monthly energy produced for the Maricopa DSCSPP, in the period between March 2010 and June 2011 (Fig. 5). It is indicated that the annual average ambient temperature and wind speed for Maricopa city, USA were 30.75 ^{o}C and 5.57 mph, respectively. While the average monthly direct solar radiation value is estimated to be 7.50 kWh/m^2/day, showing that the annual normal direct solar radiation can reach 2750 kWh/m^2/year.

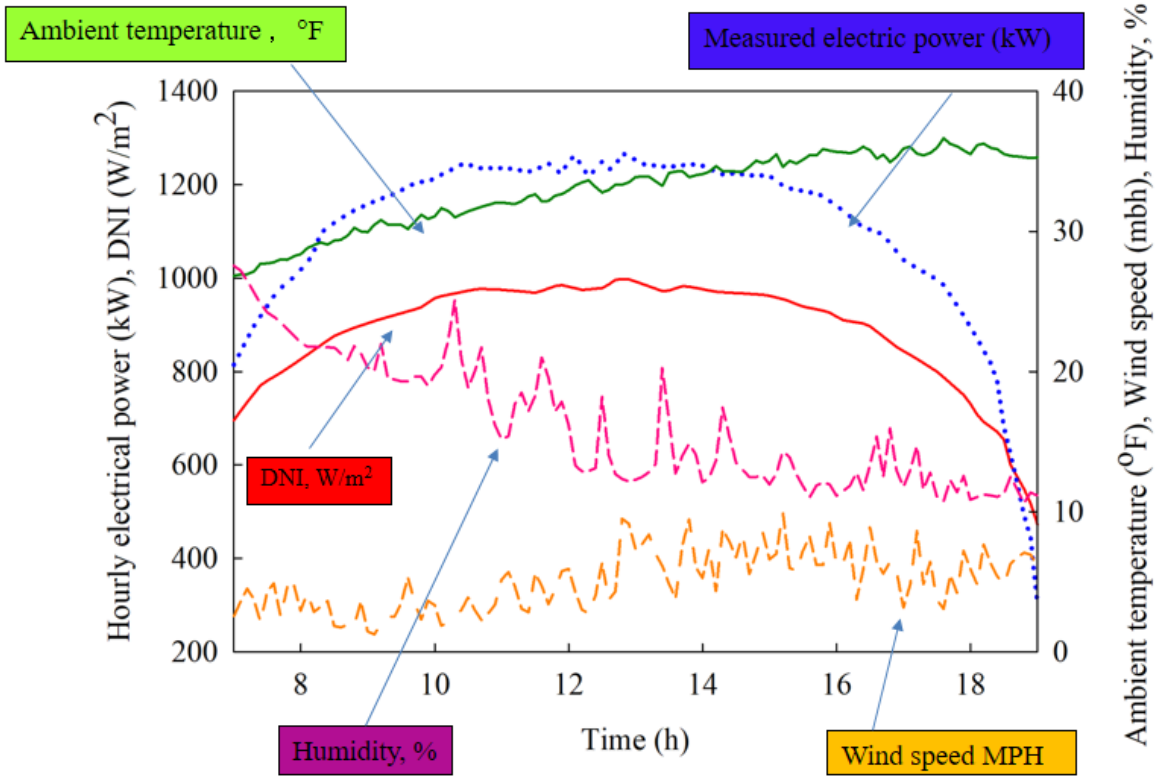

Fig. 4. Hourly climate parameters and electric power for Maricopa DSCSPP.

To study the monthly performance, the monthly variation of the predicted net average power production of the Maricopa DSCSPP is plotted in Fig. 6, in the period between March 2010 and June 2011. The results show that the high net power values of the DSCSPP are obtained between April and August, due to the temperate monsoon climate of Maricopa city, USA. It can be seen that the monthly highest energy production for the Maricopa DSCSPP was obtained in June 2010, which was achieved to be 363 MWh, whereas, the lowest energy production value of 68.2 MWh was recorded in March 2011.

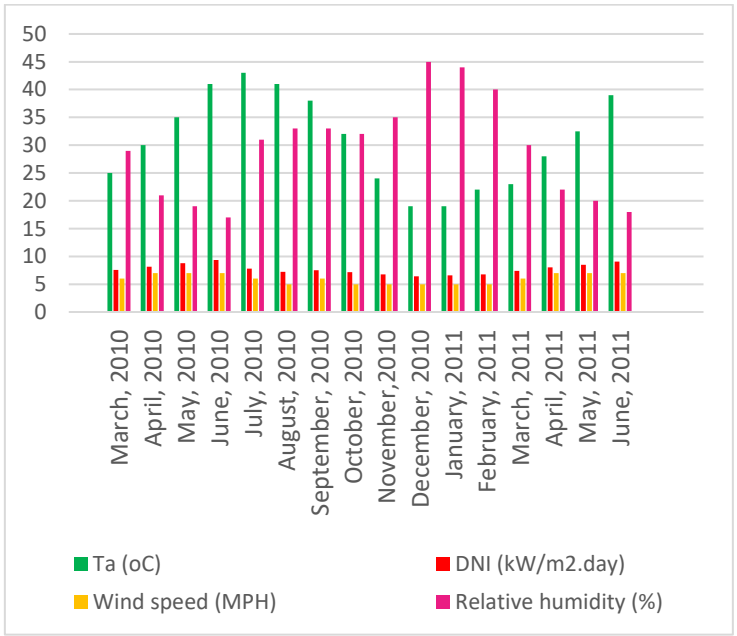

Fig. 5. Monthly average weather data levels for the Maricopa DSCSPP.

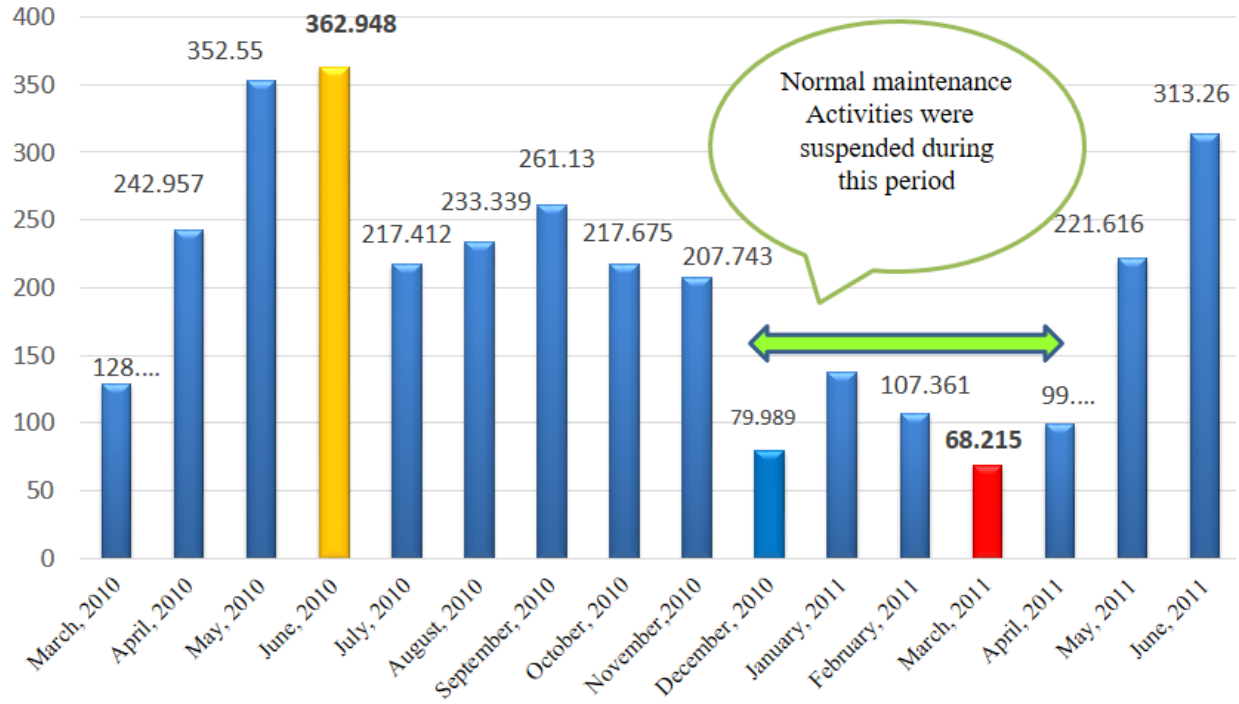

Fig. 6. Monthly energy produced for the Maricopa DSCSPP.

The simulation results obtained with the proposed DSCSPP model are validated and compared with the experimental findings of the tested DSCSPP, considering the same operating conditions and geometrical design configurations. A comparison between the experimental and theoretical findings in terms of instantaneous electrical output power and net monthly electric energy of the DSCSPP is plotted in Fig. 7 and Fig. 8. Figure 7 depicts the measured and calculated output results of the instantaneous electrical power of the DSCSPP, respectively, using the thermal analysis model. In the experiments conducted for the DSCSPP, the maximal and average measured electrical output power values are achieved as 1.267 MW and 1.107 MW, respectively. While maximal and average simulated electrical output power values of 1.24 MW and 1.09 MW, are obtained by the developed thermal model, for the DSCSPP, respectively, under the same conditions. The MAPE of the maximal and average electrical output power is 2.13% and 1.54% related to the DSCSPP, respectively. The maximum estimated absolute residual error for the predicted instantaneous electrical power results is less than 0.314 MW, respectively. These deviations in the results obtained from two different systems may be due to the absence of some design parameters in the published studies such as mirror reflectance, focal length, receiver tilt angle and Stirling coefficient. Conclusively, the comparison of the experimental results with the proposed model proves that the model had the highest performance, which is in better agreement with the measured ones.

Similarly, Fig. 8 illustrates the measured and calculated output results of the monthly electrical energy of the DSCSPP, respectively, using the thermal analysis model. It is revealed that the maximal, average, and minimal measured monthly electrical energy values are achieved as 363, 208.8, and 80 MWh, respectively. While maximal, average, and minimal simulated monthly electrical energy values of 362.95, 211.8, and 79.98 MWh, are obtained by the developed thermal model, for the DSCSPP, respectively, under the same conditions. The MAPE of the maximal, average, and minimal monthly electrical energy of the DSCSPP is 0.013%, 1.44%, and 0.025% related to the DSCSPP, respectively Also, the value of the absolute residual error for the predicted monthly electrical energy results in less than 105.35 MWh in the case of the theoretical model.

Overall, based on Fig. 10 and Fig.11, it can be recommended that the proposed thermal model is an accurate approach and can be chosen to accurately predict the hourly and monthly performance of DSCSPP and this elucidates the verification of the predicated calculations.

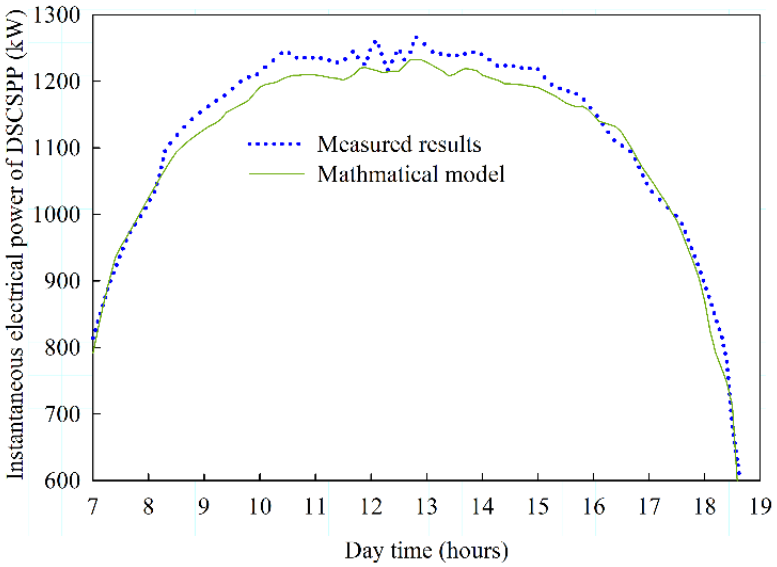

Fig. 7. Experimental and predicted hourly electrical power of DSCSPP.

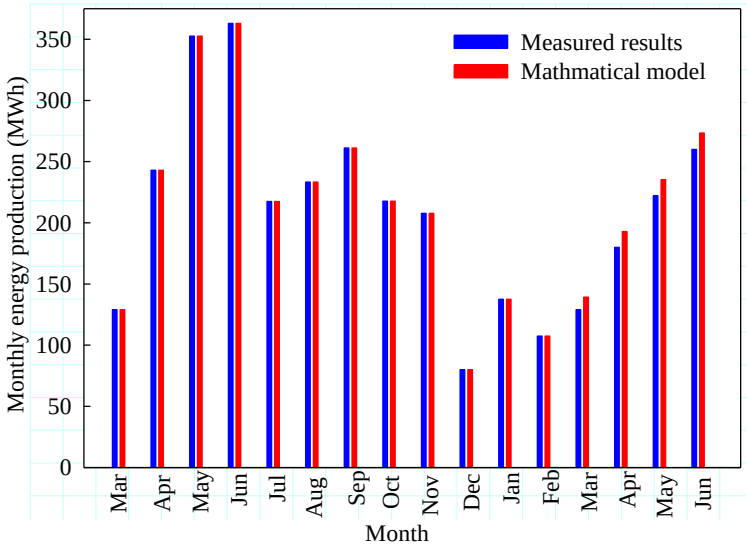

Fig. 8. Experimental and predicted monthly electrical energy DSCSPP.

Conclusion

The solar dish Stirling system has been considered one of the most promising and efficient technologies for sustainable electricity generation. This study presents an experimental analysis, technical implementation, and performance prediction of a 1.50 MW commercial dish/Stirling concentrated solar power plant (DSCSPP), installed at Maricopa Deseret, Arizona, USA (33.0581° N, 112.0476° W). A mathematical model was developed and implemented in MATLAB software to simulate the DSCSPP operation to predict and analyze its performance. Moreover, the daily, monthly, and annual performances of the DSCSPP are extensively analyzed to predict the annual electricity production and net annual efficiency of the DSCSPP. The key conclusions of this study are as follows:

1. For daily summer conditions, the DSCSPP generates a peak electric power of 1.27 MWe at a direct solar irradiance (DNI) of 998 W/m2 with an overall plant efficiency of 23.7%.
2. The monthly highest energy production for the Maricopa DSCSPP was obtained in June 2010, which was achieved to be 363 MWh, whereas, the lowest energy production value of 68.2 MWh was recorded in March 2011.
3. The proposed DSCSPP can experimentally produce 2550 MWh annually, with a yearly net overall efficiency

of 17.8%.

4. The maximal and average measured electrical output power values are achieved as 1.267 MW and 1.107 MW, respectively. While maximal and average simulated electrical output power values of 1.24 MW and 1.09 MW, are obtained by the developed thermal model, for the DSCSPP, respectively, under the same conditions. The MAPE of the maximal and average electrical output power is 2.13% and 1.54% related to the DSCSPP, respectively.

5. The maximal, average, and minimal measured monthly electrical energy values are achieved as 363, 208.8, and 80 MWh, respectively. While maximal, average, and minimal simulated monthly electrical energy values of 362.95, 211.8, and 79.98 MWh, are obtained by the developed thermal model, for the DSCSPP, respectively, under the same conditions. The MAPE of the maximal, average, and minimal monthly electrical energy of the DSCSPP is 0.013%, 1.44%, and 0.025% related to the DSCSPP, respectively.

6. Finally, it can be concluded that the present study provides new experimental and theoretical guidance for evaluating the annual performance of the DSCSPP.

Disclosure

The author reports no conflicts of interest in this work.

References

A. Buscemi, V. Lo Brano, C. Chiaruzzi, G. Ciulla, C. Kalogeri A validated energy model of a solar dish-Stirling system considering the cleanliness of mirrors. Appl. Energy, 260 (2020), 114378.

A. Khosravi, S. Syri, J.J.G. Pabon, O.R. Sandoval, B.C. Caetano, M.H. Barrientos. Energy modeling of a solar dish/Stirling by artificial intelligence approach. Energy Conversion and Management. 199 (2019) 112021.

B. Kongtragool, S. Wongwises, Optimum absorber temperature of a once-reflecting full conical concentrator of a low-temperature differential Stirling engine, Renewable Energy, 30 (2005) 1671-1687.

D. Mevada, H. Panchal, M. Ahmadein, M.E. Zayed, N.A. Alsaleh, J. Djuansjah, E.B. Moustafa, A.H. Elsheikh, K.K. Sadasivuni, Investigation and performance analysis of solar still with energy storage materials: An energy- exergy efficiency analysis, Case Studies in Thermal Engineering, 29 (2022) 101687.

G. Caballero, Mendoza L.S , A.M. Martinez, E.E. Silva, V.R. Melian, O.J. Venturini, O.A. del Olmo, Optimization of a Dish Stirling system working with DIR-type receiver using multi-objective techniques, Applied Energy, 204 (2017) 271-286.

Holman, J.P., 2012. Experimental methods for engineers.

J. Coventry, C. Andraka. Dish systems for CSP. Solar Energy. 152 (2017) 140-70.

L. Jing, J. Zhao, H. Wang, W. Li, Y. Du, Q. Zhu, et al. Numerical analysis of the effect of swirl angle and fuel equivalence ratio on the methanol combustion characteristics in a swirl burner. Process Safety and Environmental Protection. 158 (2022) 320-30.

M. Alata, M.A. Al-Nimr, Y. Qaroush. Developing a multipurpose sun tracking system using fuzzy control. Energy Conversion and Management. 46 (2005) 1229-45.

M. Castellanos, A.L. Galindo Noguera, G.E. Carrillo Caballero, A.L. De Souza, V.R. Melian Cobas, E.E. Silva Lora, O.J. Venturini, Experimental analysis and numerical validation of the solar Dish/Stirling system connected to the electric grid, Renewable Energy, 135 (2019) 259-265.

M. E. Zayed, Zhao, J., Elsheikh, A. H., Zhao, Z., Zhong, S., Kabeel, A. E. Comprehensive parametric analysis, design and performance assessment of a solar dish/Stirling system. Process Safety and Environmental Protection, 146, (2021). 276-291.

M.E. Zayed, J. Zhao, A.H. Elsheikh, W. Li, M.A. Elaziz, Optimal design parameters and performance optimization of thermodynamically balanced dish/Stirling concentrated solar power system using multi-objective particle swarm optimization, Applied Thermal Engineering, 178 (2020) 115539.

M.E. Zayed, J. Zhao, A.H. Elsheikh, W. Li, S. Sadek, M.M. Aboelmaaref. A comprehensive review on Dish/Stirling concentrated solar power systems: Design, optical and geometrical analyses, thermal performance assessment, and applications. Journal of Cleaner Production. (2020) 124664.

M.E. Zayed, J. Zhao, W. Li, A.H. Elsheikh, A.M. Elbanna, L. Jing, et al. Recent progress in phase change materials storage containers: Geometries, design considerations, and heat transfer improvement methods. Journal of Energy Storage. 30 (2020) 101341.

M.E. Zayed, J. Zhao, W. Li, A.H. Elsheikh, Z. Zhao, A. Khalil, et al. Performance prediction and techno-economic analysis of solar dish/Stirling system for electricity generation. Applied Thermal Engineering. 164 (2020) 114427.

M.E. Zayed, V.P. Katekar, R.K. Tripathy, S.S. Deshmukh, A.H. Elsheikh, Predicting the yield of stepped corrugated solar distiller using kernel-based machine learning models, Applied Thermal Engineering, 213 (2022) 118759.

M.H. Ahmadi, S.S.G. Aghaj, A. Nazeri. Prediction of power in solar stirling heat engine by using neural network based on hybrid genetic algorithm and particle swarm optimization. Neural Comput Appl. 22 (2013) 1141-50.

M.M. Aboelmaaref, M.E. Zayed, A.H. Elsheikh, A.A. Askalany, J. Zhao, W. Li, et al. Design and performance analysis of a thermoelectric air-conditioning system driven by solar photovoltaic panels. Proceedings of the Institution of Mechanical Engineers, Part C: Journal of Mechanical Engineering Science. (2020) 0954406220976164.

M.M. Aboelmaaref, M.E. Zayed, J. Zhao, W. Li, A.A. Askalany, M. Salem Ahmed, et al. Hybrid solar desalination systems driven by parabolic trough and parabolic dish CSP technologies: Technology categorization, thermodynamic performance, and economical assessment. Energy Conversion and Management. 220 (2020) 113103.

NREL. Maricopa Solar Project. https://solarpacesnrelgov/maricopa-solar-project. (2016).

P.R. Steinfeld A, Solar thermochemical process technology., Encyclopedia of physical science and technology;, (2003) 237–256.

R. Almodfer, M.E. Zayed, M.A. Elaziz, M.M. Aboelmaaref, M. Mudhsh, A.H. Elsheikh, Modeling of a solar-powered thermoelectric air-conditioning system using a random vector functional link network integrated with jellyfish search algorithm, Case Studies in Thermal Engineering, 31 (2022) 101797.

R. Beltrán-Chacon, D. Leal-Chavez, D. Sauceda, M. Pellegrini-Cervantes, M. Borunda, Design and analysis of a dead volume control for a solar Stirling engine with induction generator, Energy, 93 (2015) 2593-2603.

R. Loni, E.A. Asli-Ardeh, B. Ghobadian, M.H. Ahmadi, E. Bellos. GMDH modeling and experimental investigation of thermal performance enhancement of hemispherical cavity receiver using MWCNT/oil nanofluid. Solar Energy. 171 (2018) 790-803.

R.Y.Ma, Wind Effects on Convective Heat Loss from a Cavity Receiver for a Parabolic Concentrating Solar Collector,, Sandia, (1993).

S. Guarino, A. Buscemi, G. Ciulla, M. Bonomolo, V. Lo Brano. A dish-stirling solar concentrator coupled to a seasonal thermal energy storage system in the southern mediterranean basin: a cogenerative layout hypothesis. Energy Convers Manage, 222(2020), 113228.

S.A. El-Agouz, A.R. Abd Elbar, A.M. Aboghazala, M. Shahin, M.Y. Zakaria, K.K. Esmaeil, et al. Comprehensive parametric analysis, sizing, and performance evaluation of a tubular direct contact membrane desalination system driven by heat pipe-based solar collectors. Energy Conversion and Management. 274 (2022) 116437.

S.A. El-Agouz, M.E. Zayed, A.M. Abo Ghazala, A.R.A. Elbar, M. Shahin, M.Y. Zakaria, et al. Solar thermal feed preheating techniques integrated with membrane distillation for seawater desalination applications: Recent advances, retrofitting performance improvement strategies, and future perspectives. Process Safety and Environmental Protection. 164 (2022) 595-612.

S.M. Shalaby, A. Khalil, A.E. Kabeel, M.E. Zayed. Improvement of the Thermal Performance of the v-Corrugated Plate Solar Air Heater with PCM by Using Insulated Upper Cover during Night. 2018 IEEE International Conference on Smart Energy Grid Engineering (SEGE) 2018. pp. 346-50.

SES. Stirling Energy Systems Co. http://wwwstirlingenergycom/projects/indexhtml. (2015).

Steinfeld S., M. Schubnell, Optimum aperture size and operating temperature of a solar cavity-receiver, Solar Energy, 50 (1993) 19-25.

T. Mancini, P. Heller, B. Butler, B. Osborn, W. Schiel, V. Goldberg, et al. Dish-Stirling Systems: An Overview of Development and Status. Journal of Solar Energy Engineering. 125 (2003) 135-51.

V. Siva Reddy, S.C. Kaushik, S.K. Tyagi. Exergetic analysis and performance evaluation of parabolic dish Stirling engine solar power plant Int J Energy Res, 37 (11) (2013), pp. 1287-1301.

V.T. Morgan, The Overall Convective Heat Transfer from Smooth Circular Cylinders, in: T.F. Irvine, J.P. Hartnett (eds.) Advances in Heat Transfer, Vol. 11, Elsevier, 1975, pp. 199-264.

Z. Li, D. Tang, J. Du, T. Li, Study on the radiation flux and temperature distributions of the concentrator–receiver system in a solar dish/Stirling power facility, Applied Thermal Engineering, 31 (2011) 1780-1789.